IOWA STATE UNIVERSITY
Digital Repository

2020

Additive printing for civil infrastructure: Assessing concrete mix design, printability and nozzle effects

Karthick Manikandan Gopalakrishnan Deivanai
Iowa State University

Additive printing for civil infrastructure: Assessing concrete mix design, printability and nozzle effects

by

Karthick Manikandan Gopalakrishnan Deivanai

A thesis submitted to the graduate faculty

in partial fulfillment of the requirements for the degree of

MASTER OF SCIENCE

Major: Industrial Engineering

Program of Study Committee:
Hantang Qin, Major Professor
Matthew Frank
Beiwen Li

The student author, whose presentation of the scholarship herein was approved by the program of study committee, is solely responsible for the content of this thesis. The Graduate College will ensure this thesis is globally accessible and will not permit alterations after a degree is conferred.

Iowa State University

Ames, Iowa

2020

DEDICATION

To my loving parents, Mr. P. Gopalakrishnan, Mrs. K. Theivanai, and my endearing

brother G.D.Vignesh

TABLE OF CONTENTS

LIST OF FIGURES

vii

LIST OF TABLES

Page

ACKNOWLEDGMENTS

I would like to thank my committee chair Dr. Hantang Qin and Dr. Kejin Wang from the Civil engineering department for their guidance and support throughout this research.

I would like to thank my committee members Dr. Beiwen Li and Dr. Matthew Frank for serving on my committee,

Also, I would like to thank Dr. Xiaolei Shi, Mr. Aaron Jordan (Lab Supervisor), Kwangwoo Wi, Department of Transportation-Ames, Iowa Highway Research Board, and the IMSE department faculty and staff, for making my time at Iowa State University a wonderful experience.

This research study was based upon work supported by the Innovative Project Program from Iowa Department of Transportation (Iowa DOT TR-756) and the Undergraduate Research Assistant Program from the Department of Industrial and Manufacturing Systems Engineering (IMSE_URA) at Iowa State University. Their supports to carry out this work is greatly appreciated.

ABSTRACT

The need to automate the construction process for civil infrastructures has been perpetually propelled by the reported number of detrimental site accidents, enormous time, and material wastages in the current labor-intensive approaches. Additive 3D printing applications in the construction sector could revolutionize the construction sites. The 3D printing technologies will be an eco-friendly variant and will relax the formwork requirement, giving wider build customizability when compared to the traditional construction methods. The notable advantages of 3D printing over conventional construction techniques include safer work ambiance, reduced cost, and time for construction.

The first objective of this research work is to identify the concrete mixture that is readily available for 3D printing and establish their material characteristics. This work serves up a model schema for researchers to look up and identify desired mixture properties for instantaneous concrete printing. In this study, ready-to-print fresh cementitious mixtures were characterized for printability and buildability based on their rheological and mechanical properties. Admixtures such as Silica fume and Superplasticizer were added to the ordinary Portland cement in different proportions to test and improve the yield stress and attain the desired viscosity for 3D printing.

The other objective is to study the impacts of using different nozzle geometries in the printed constructs. In the additive 3D printing process, choosing the right nozzle geometry before printing is critical as it affects the surface finish as well as the mechanical properties of the constructs. This study utilizes point cloud data of the printed samples obtained from Structured Light System- a scanning technique to measure the contour deviation and surface roughness. The compression strength of the mixtures was determined to explore the mechanical properties, by conducting compression tests as per the ASTM standards. A comparative study on the compression

strength of 3D printed constructs with precast was made to identify the impacts of nozzle geometry in the compression strength.

To summarize, a concrete extrusion system has been built and the concrete flow properties that are desirable for instantaneous 3D printing have been identified. The rheological properties, printability, and buildability of all the identified concrete mixtures were evaluated and the best mixture proportions were advanced for printing constructs. The nozzle geometry study has established the impacts on the contour as well as the mechanical properties on the constructs, and hence urging the need to choose the right nozzle geometry before 3D printing.

CHAPTER 1.   INTRODUCTION

In today's construction field, concrete is one of the globally used materials as they are highly beneficial for both in-situ construction and prefabrication. Concrete provides a better moldability, thermal resistance, and durability under a relatively lower production cost. Although concrete has the innate material advantages, it requires higher labor activities starting from mixing with appropriate admixtures, casting to the required shape (Formwork), until temperature-controlled curing for desired mechanical properties. According to a recent study [1], a formwork can account for about 50% of the total construction cost and takes about 70% of the construction time. The cost would be increased if the construction design is intricate. The other challenge is to handle the substantial amount of waste generated from the construction sites since frames are difficult to recycle after casting concrete [2]. According to the Environmental Protection Agency (EPA), about 578 million tons of construction and demolition debris was generated in the year 2015 in the United States [3]. The next major challenge is the reported number of accidents and fatalities in the construction sites. Occupational Safety and Health Administration (OSHA) reported that 20.7% of the fatalities (about 1000 deaths) in the private industries happened at construction sites in the United States in 2017 [4].

The construction industry has gone through numerous automation, specifically, single robotic arms deployed in the early 1980s reduced the labor activities on construction sites [5]. Although semi-automated and automated machines were introduced to handle the cementitious and other construction materials, the need for labors on site has not diminished. 3D printing a constructive approach has attracted attention from various fields due to its advantages such as easy customization, efficient material consumption, less human-machine interaction, and relatively less production time [6]. For the past few years, researchers across the countries looked up the 3D

printing process as a technological revolution in the construction field as it could reduce the material wastage, and labor activities thereby reducing the production cost and fatalities on the construction sites.

1.1. Background and Literature on 3D Printing

3D printing is an additive manufacturing technique in which parts are constructed in a layer-by-layer fashion. The process starts with the 3D Computer-Aided Design (CAD) model of the required part which is then converted into a Standard Tessellation Language (STL) file format which has the coordinate information of the object or part boundaries. This conversion of a 3D CAD model into an STL file is done by a process called tessellation. For 3D printing, the object surface is tiled (tessellated) with triangular planes and hence STL is also known as Standard Triangulated Language. The tessellated or triangulated object is then sliced into layers with the equal layer height. The sliced layers are then converted into the G-codes that have the toolpath information for printing. Figure 1 below shows the flow diagram of the 3D printing process.

There are several 3D printers available on the market that work on different principles say for example Stereolithography, Selective Laser Melting, Direct Metal Laser Sintering used for a range of metals, and plastics.
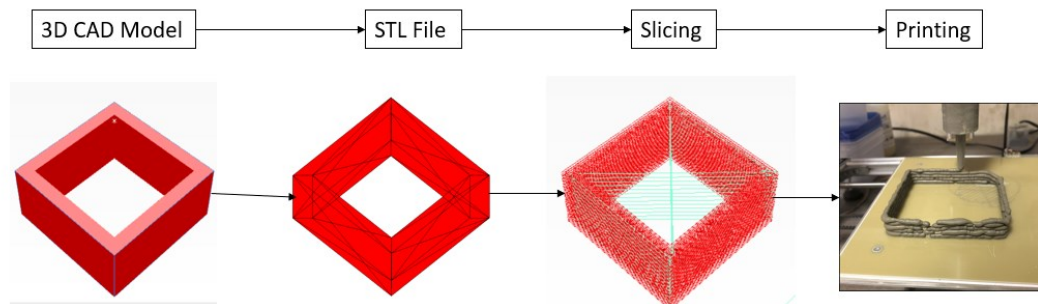
Figure 1. 3D printing process flow diagram

The extrusion-based printers are more commonly used due to the numerous Do-It-Yourself (DIY) toolkits and open source software available to construct as well as to control the printers [7].

Based on the literature on 3D printers in the construction industries, the concept of "3D printer for concrete" was first introduced by a research group at the University of Southern California to solve common problems caused by the conventional concrete construction [8]. The 3D printing technology for construction and concrete has been developed in different ways including Contour Crafting [9], CONPrint3D [10], and Large-Scale 3DCP using Ultra-High-Performance Concrete [11]. Hinczewski et al [12] developed a Stereolithography printer to print ceramic parts, Liang [13] constructed an FDM based printer to print an entire house, Gibson et al [14] utilized FDM and SLS techniques to print architecture models and those printers used sand and clay apart from cementitious mixtures. Contour Crafting and D-Shape processing are the three most used large-scale additive printing processes involved in construction and building domains [15]. While 3D printing provides mass customization and the construction industry considered as an industry with a low degree of customization, meaning the ability to customize the shapes of constructs using cement is very low, the researchers can work with wide choices of 3D printing techniques and various mixtures and compounds for constructions [16]. This technology is recently gaining more popularity from different countries and companies for its reasons and benefits. The government of Singapore has a plan to build public housing with a strategy of the Prefabricated Prefinished Volumetric Construction (PPVC) [17]. PVVC is a large-scale 3D printer that prints concrete without the need for casting in the field. Another type of printer variant known as binder jetting which is a powder-based printer. It uses a binder (glue) to bind the layers to develop the parts. Binder is ejected/sprayed on a thin layer of powder material spread on the substrate. The

binder acts as adhesion and binds with the powder. The parts that are printed out of the Binder Jetting technique will be slightly bigger than the required dimensions as the binder occupies a proportionate space while printing the layer. Hence in this process, a required allowance/tolerance should be provided for the binder [18]. The interlaminate strength between the layers completely depends on the nature of the binder used to construct the part/component. Higher the penetration of binder into the powder, the higher is the strength of the part [19]. In the building and construction industry Voxel jet and Monolite printers work under this additive printing principle to print architectural components using sand mixtures [20]. Printers that follow Material Deposition Method have either a huge gantry or a multi-axis robotic arm [21] which enables printers to print a large-scale object or a complex structure. The Singapore Centre for 3D (SC3DP) printing utilized a 6-axis robotic arm printer constructed by Wolf [22]and a four-axis gantry printer [23] for 3D printing the fiber-reinforced mortar. SC3DP [24] concluded by saying that the gantry-based printers are suitable for large-scale printing whereas the robotic arm-based printers are more suitable for complex structural objects.

1.2.Basic Requirements for a Concrete Printer

The basic principle of the proposed 3D concrete printer is to extrude the concrete mixture through a nozzle and deposit on the build plate (ground) as per the part geometry requirement. Compared to the traditional concrete construction, the difference is that the concrete must be extrudable (extrudability) and must retain specific rheological properties desired for stacking up the layers. The next chapter in this thesis will discuss more the rheological properties in detail. Generally, the concrete should flow from the nozzle, and get hardened right after it is extruded without any external support. From the rheological view, the concrete mixture should have high yield stress and relatively low viscosity so that it can be extruded out of the nozzle and cured

spontaneously. However, normal Portland cement does not have these characteristics at the same time. For this reason, admixtures such as viscosity modifiers are used in different proportions to fulfill the requirements. Several researchers have tried to use several types of admixtures to achieve extrudability [25-29]. Most of those research works are associated with transporting the ready-to-pour concrete mixtures to the construction sites. The admixtures added to the cement mix should reduce the suspension associated with extrusion, the phenomenon during which the water flows out leaving the other mixtures inside the printer. On the other hand, if the concrete hardens rapidly inside the extruder, it will block the nozzle and leads to discontinuity while printing.

Another important discussion on concrete printing is the interlaminar bond strength of the fabricated part. The interlaminar bond strength of the printed part purely depends on the area of contact between the layers and the physical and chemical properties of the concrete. When printed, the area of contact of concrete between the successive layers depends on the shape of the extruded filament. The shape of the extruded filament depends on the shape of the print heads/nozzles. Therefore, it is also crucial to study the geometry of the nozzle, as it directly affects the interlaminar strength and the surface finish of the constructs. Theoretically, in the case of a circular filament, extruded from a circular nozzle, there will be a single point of contact between the layers and in case of rectangular or square filament, from rectangular or square-shaped nozzle there will be a higher area of contact. Figure. 2 below shows the difference in the theoretical contact areas for rectangular and circular filaments.
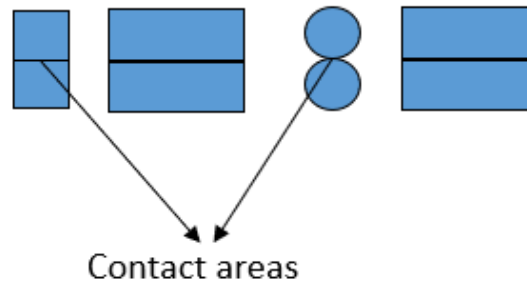
Contact areas

Figure 2. Theoretical contact areas for rectangular and circular filaments

Bos et al. [6] reported that the square and rectangular-shaped nozzles printed stable shapes than the circular nozzles due to the higher contact area. Wolfs et al. [30] reported the technical difficulty in using the square and rectangular nozzles. The print head should rotate through 90 degrees at the corners accurately to print closed loops, and if failed, the print head generates a flip or twists on each layer. Also, in the case of rectangular nozzles, the dimensions of the printed zone vary drastically than the other nozzles. To achieve this 90-degree rotation, the versatility of the printer should be taken into consideration. [31] reported that the extruder with a square nozzle yielded better surface finish to the printed parts rather than the ellipse/circular nozzles. As an extension of these nozzle studies, this research work would quantify the contour deviations and surface roughness of the printed constructs while using circular and square nozzle heads.

This thesis has been structured into the following sections: Chapter 2 runs through constructing a novel desktop-based 3D concrete printer that follows the Material Extrusion (ME) principle and identifying concrete mixture proportions and sample preparations to test the extrudability and buildability. Chapter 3 and 4 cover the Concrete mix characterization based on the rheological and compression tests, the test results were summarized and a model chart to identify the best concrete mix was given. Chapters 5 and 6 discuss the impacts of using square and

circular nozzle geometries in the contour deviation, surface roughness, and compression strength of the 3D printed constructs.

CHAPTER 2.   PRINTING PLATFORM AND CEMENT MIXTURE DESIGN

This research study intends to build a concrete printer based on the direct material extrusion (DME) principle and identify the appropriate cement and additives mixture proportions to 3D print concrete constructs. In the proposed DME system, the freshly prepared concrete paste is extruded using a syringe. For this system, the rheological properties of the concrete mixture should favor both the buildability and the printability. The term buildability in concrete 3D printing refers to the ability of the mixture to stack up the layers. Quantitatively, the buildability of a concrete mixture is defined as the number of layers it could hold up until the structure collapse or a noticeable deformation. Y. Weng et al [32] suggested that the concrete mixture should hold high yield stress for good buildability. As mentioned earlier, admixtures such as fly ash, silica fume, sand, and other chemical agents were mixed with cement to increase the printability of the mixture which also impacts yield stress. The printability of the concrete is a state during when the concrete mixture holds the desirable range of viscosity over a period and the mixture can be extruded out of the nozzle under the constant extrusion force. To extrude the equal quantity of the mixture while printing the viscosity of the mixture should be controlled. Researchers have also utilized Viscosity Modifying Agents (VMAs) such as Superplasticizers (SP) and organic cellulose to get the favoring viscosity for their concrete mixtures. This study involves identifying the perfect balance between the yield stress and the viscosity with which the mixture can be prepared and printed with ease.

2.1. Printing Platform and Concrete Additives

An extrusion-based Velleman K8200 3D printer was constructed in the lab (Figure. 3) to instantly test the printability of the concrete mixtures. The resolution in the x and y-axis was 0.015mm, resolution in the z-axis was 0.0019mm. The maximum printing speed is 300mm/s. The printable area was: 200x200x200mm. The printer can print up to 60mm of concrete layers. A 3mm

diameter nozzle was fixed constantly. The travel speed and the feed rate in the printer can be adjusted and were maintained at 65 and 25mm/s respectively throughout the experiments. With these results alongside the printed concrete constructs, a standard chart has been proposed. This standard chart (Table: 1) has both the rheological properties (Yield stress, thixotropy, and viscosity) and the printability discussion about all the mixtures identified. Based on this standard chart, the researchers can interpolate the best concrete mixture composition for concrete 3D printing.

A regular type II Portland cement, polycarbonate superplasticizer, and silica fume were mixed in six different proportions, as shown in Table 1. The water-to-cement (W/C) ratio was kept constant for all the mixtures as 0.3 based on manual extrusion trials that were suitable for the laboratory printing. Studies [33-35] revealed that the superplasticizer added in the mixture improved the flowability and acted as a viscosity modifying agent (VMA). To enhance the cohesion and the mechanical properties of the mixture, densified silica fume was added as a supplementary concrete mixture (SCM) [36,37].

2.2.Sample Preparation and Testing Parameters

A standard mixing procedure was followed for sample preparation, as many factors such as mixing additives, proportion, and mix time, affect the rheological properties. Firstly, the solid additives (cement and silica fume) were dry mixed for 3 minutes followed by mixing with 50% (w/w proportion) of water and superplasticizer (SP) for 5 minutes at constant stir speed. All the samples were hand-mixed. The sample preparation procedure was kept the same for both rheological assessments as well as printing.

Table 1. Cement, silica fume, superplasticizer and water mixture proportions

W/C ratio	Cement (g)	Silica Fume (g)	Superplasticizer (g)	Water (g)
0.3	95	5	1.5	28.5
	97.5	2.5	1.5	29.25
	200	0	1.5	30
	95	5	2.5	28.5
	97.5	2.5	2.5	29.25
	200	0	2.5	30

2.1. Concrete Printer Construction

The functional layout of the proposed desktop-based concrete printer is shown in figure 3 below. In the direct material extrusion system, the extruder is mounted in a gantry that moves up and down completing Z-axis and the substrate of the printer is actuated in X and Y directions. The extruder, X, Y, and Z motions of the printer are actuated by the DC motors which are controlled synchronously by an Arduino microcontroller. The substrate temperature was maintained at room temperature. Attempts made to heat the substrate resulted in developing cracks in the printed layers.
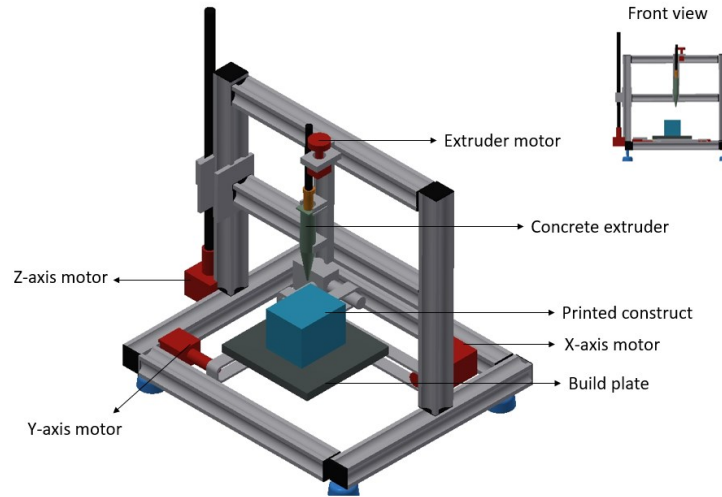
Figure 3. Proposed concrete printer layout

CHAPTER 3.   CONCRETE MIX CHARACTERIZATION FOR 3D PRINTING

3.1.Rheological Properties

Rheology is a study of flow behavior, in which the fluid deformation is measured under the applied strain rate. The rheological flow ramp assessment of all the concrete mixtures given in Table 1 was conducted to understand their flow characteristics. During the assessment, the concrete mixtures showed the properties of a non-Newtonian fluid. The yield stress and the apparent viscosity of the concrete mixtures were evaluated from the shear stress vs. shear rate plot obtained from the tests. All the rheological tests were conducted in a closed chamber by continuously varying the shear rate. The rheological assessments of the mixtures were done on the Discovery Hybrid rheometer, TA instruments shown in figure 4.
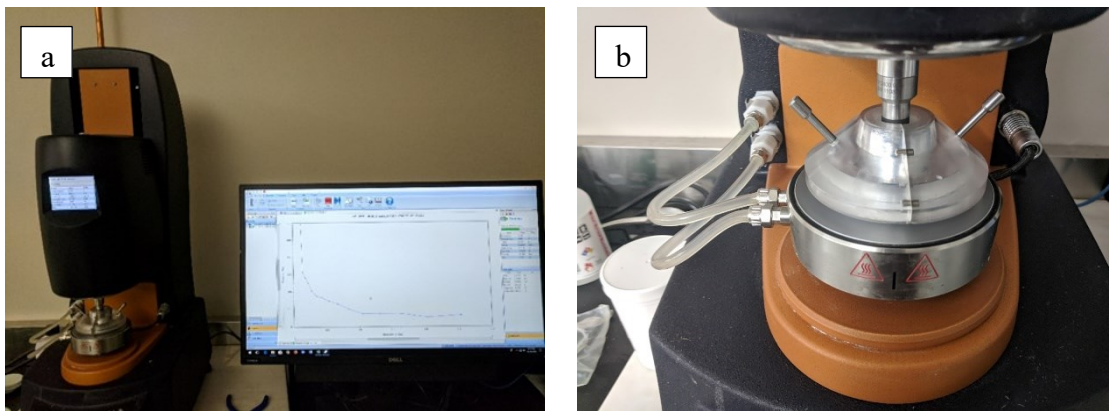
Figure 4. a) Discovery hybrid rheometer b) Closed chamber cylindrical serrated plates

All the six samples were loaded on to the rheometer and allowed to soak for 120 seconds so that they regain the shear properties which they lost while mixing. The following parameters were set in the rheometer to obtain the rheograms: 1) Strain rate: 0.1 to 100 s^{-1}; 2) Loading: 0.1 to 100 s^{-1} and Unloading 100 to 0.1 s^{-1}; time: 5 minutes for loading and unloading 3) Dwell time between loading and unloading: 1 minute; 3) Geometry: Ø40 mm parallel plates; and 4) Gap size:

1200µm. The loading and unloading were carried out three times on fresh samples for all six mixtures to ensure repeatability of the experimental data.
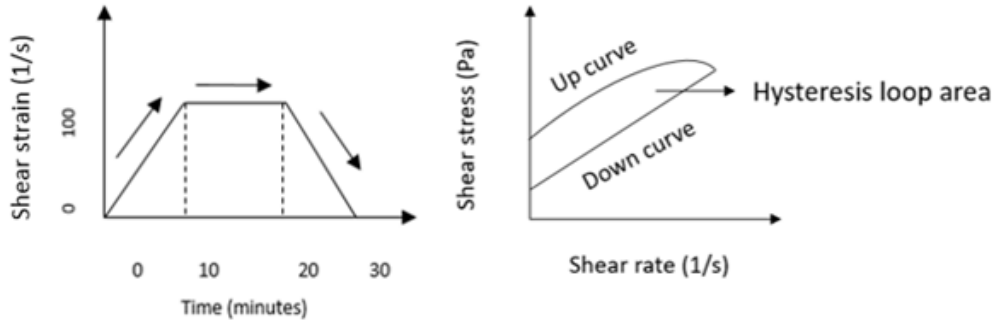
Figure 5. Loading conditions and the expected rheogram plot

Thixotropy is a collective term for a series of events and can be defined as follows: the structural breakdown of the mixtures when shearing and the eventual restructuration of mixtures at rest. The thixotropic behavior of cementitious materials can be considered as the coagulation of mixture particles when there is no shearing load applied. Once the external shearing is applied to the mixture, the microstructures breakdown, and the particles are separated. This reversible coagulation, separation, and re-coagulation of the cementitious mixture are measured as the thixotropic index of the samples. The rheological flow ramp assessment can be compared with the cement mixture being extruded out from the print head. Under the applied force, the mixture should squeeze out of the extruder showing less yield stress and once they are out, the material regains the viscosity thus start solidifying.

The yield stress and the plastic viscosities of the mixtures were interpolated by relating the down curves with the Bingham plastic model using the following equation

$$\tau = \tau_0 + \mu \dot{\gamma} \text{ .... (1)}$$

Where τ = Shear stress; τ_0 = Yield stress; μ = Apparent viscosity; $\dot{\gamma}$ = Strain rate

The thixotropy index (the area between the up curve and down curve) was calculated for all the mixtures by measuring the area between the loop formed, whereas the apparent viscosities of the mixtures were measured and noted at the shear rates 10, 50 and 80s^{-1}.

3.2. Compression Test

The compression test is one of the most conventional tests used to characterize the mechanical properties of a mixture/ink. This test aims to identify the compressive strength of all the six identified mixtures and perform a quantitative study on the mechanical strength of the cement when mixed with superplasticizer and silica fume at different proportions. To determine the compressive strength of each mixture the samples were tested in Shimadzu UH-F300kNX hydraulic universal testing machine (UTM) as per ASTM C39/39M [38]. The cylindrical molds (2"x 1") are 3D printed using Uprint- a polymer printer and the molds are filled with the cementitious mixture and compacted. The samples are mixed as per the requirements of ASTM C192/192M [39].
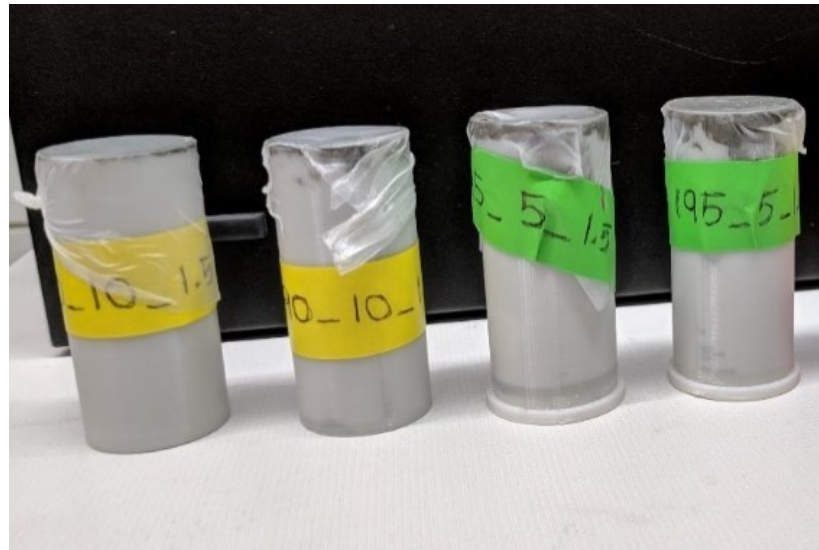
Figure 6. Cement mixture castings

The molds were stripped off after 2 days with a tolerance of ±2 hours and the specimens were kept exposed to room temperature for 1 day before testing. The samples were loaded in the UTM until failure without any shock loading. The ultimate load until failure was noted for all the samples and were used to calculate the compression strength of the mixtures using (2).

$$F_{comp} = \frac{4P_{max}}{\pi D^2}$$ ……………………………………… (2)

Where Pmax = the ultimate load [lbf], and

Fcomp = compressive strength of the mixture [psi], and

D = diameter of the sample [in]

A set of three samples for each mixture were prepared and tested to ensure the repeatability and the reliability of the results. For all the 18 samples according to the ASTM C39/39M standards, a type 3 columnar vertical cracking with no cones kind of failure was noted. The test results align well with the single operator COV values of the standards as the range of compression strength of all the samples are in between 2800 to 7500 psi.

Figure 7. a) Cement cast failed in the UTM machine b) Type 3 columnar vertical cracking

CHAPTER 4.   MIX CHARACTERIZATION TEST RESULTS

4.1.Rheology Test Results

The rheology test results are shown in the figures 8-11 below. The concrete mixtures displayed the properties of a non-Newtonian fluid, and they corresponded well with the Bingham plastic model. It can be seen from the shear rate vs shear stress plot that for all the mixtures, the viscosity increases with the increase in the shear rate, and once when the applied shear rate is taken off the mixture regains the viscosity. This confirms the thixotropic property of the mixture. Several kinds of research on rheological properties of different concrete mixtures were made before to determine the flowability and buildability, however, thixotropy of concrete mixture has not been explored yet. Shear thickening of concrete mixtures with mineral additives was reported in [40], [41] investigated the rheological characteristics of concrete under high pressure, [42] studied the effects of different superplasticizers on the rheological properties of the concrete. [43-45] utilized the rheological assessment to study the flow characteristics of the concrete. To establish that relation, three parameters, namely apparent viscosity, yield stress, and thixotropic index values, were evaluated from the rheograms of all the mixtures. Researchers [46-48] have utilized the hysteresis loop area derived from the rheological assessment as a good estimator of the thixotropic behavior of the mixtures. To calculate the yield stress of the samples, the down curves of the experiments were fitted with the Bingham model and the yield stresses are estimated using equation 1. The up and down curves in the thixotropic curve explain the de-structuration of the concrete whereas the area between the curve explains the re-structuration of the mixture. The re-structuration of the mixture corresponds to the ability of the mixture to solidify once extruded and gain back the yield stress to hold the next layer up. Whereas the de-structuration of mixture correlates to the ability of the mixture to breakdown and flow out of the nozzle. The rheological

flow ramp test was designed in such a way that all the samples are soaked for a period of 120 s to regain the viscosity back which they lost while mixing the sample preparation. The sample preparation involved in continuous agitation of the ingredients and hence the mixture would display reduced yield stress. During this soaking time, the mixture gains them back and this increases the accuracy of the measured data (Yields stress and viscosity) from the rheometer. It can be seen from the estimated yield stress values that, the addition of the silica fume to cement has increased the yield stress which is required for the structuration. The silica fume has the property to reduce the mobility of the water (bleeding) within the concrete as they have a higher surface area. This also increases the printability for the mixture as adding silica fume holds the water and the mixture together rather than just the water being dispelled out of the nozzle. The addition of superplasticizer has increased the workability of the mixture which can be seen from the mini-slump test. Based on the results obtained from the rheology tests the mixture with appropriate viscosity and the yield stress has been prioritized for printing.
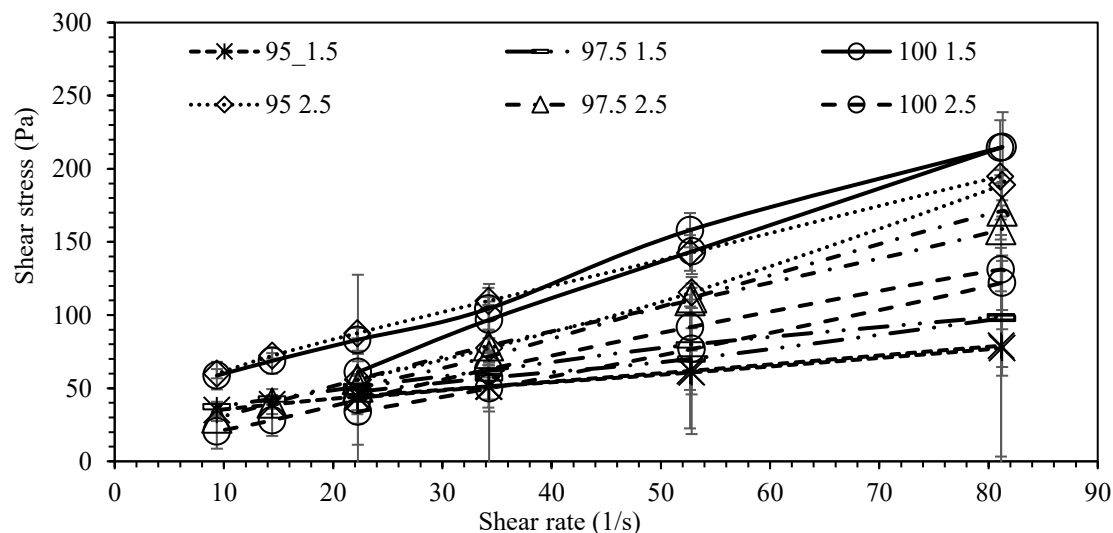

Figure 8. Up and down curves - Rheograms for the mixture
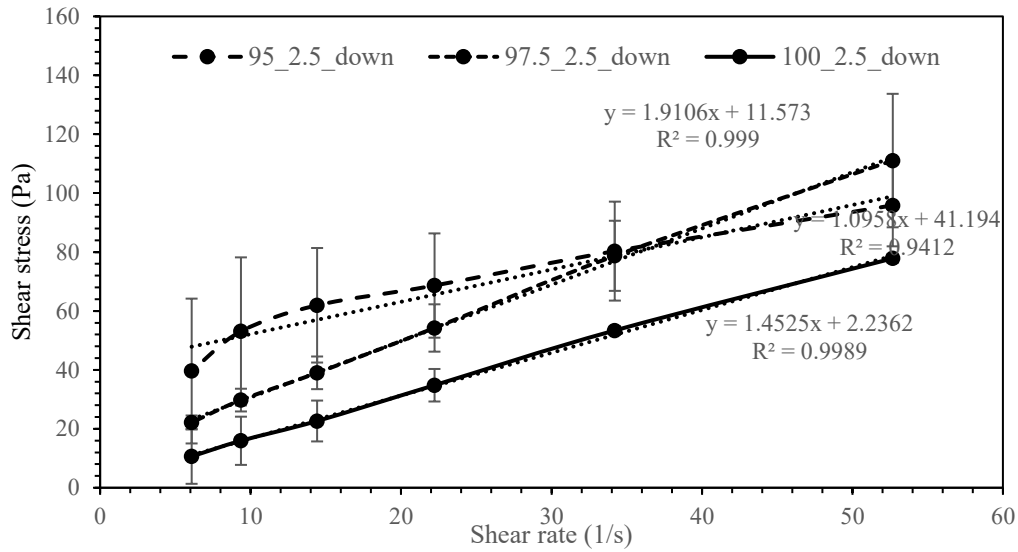
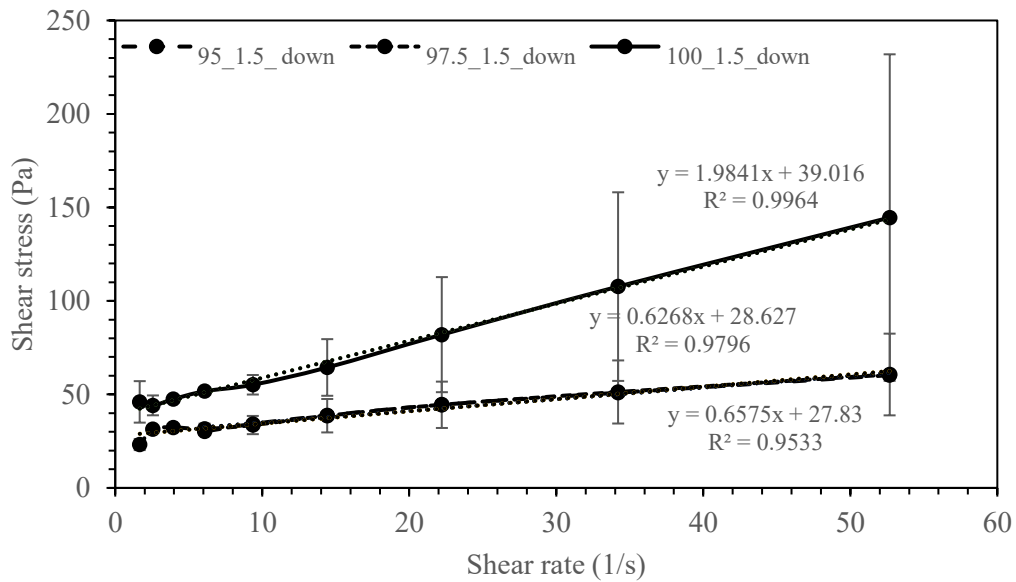Figure 9. Down curves for all the mixtures with 2.5 grams of superplasticizer

Figure 10. Down curves for all the mixtures with 1.5 grams of superplasticizer
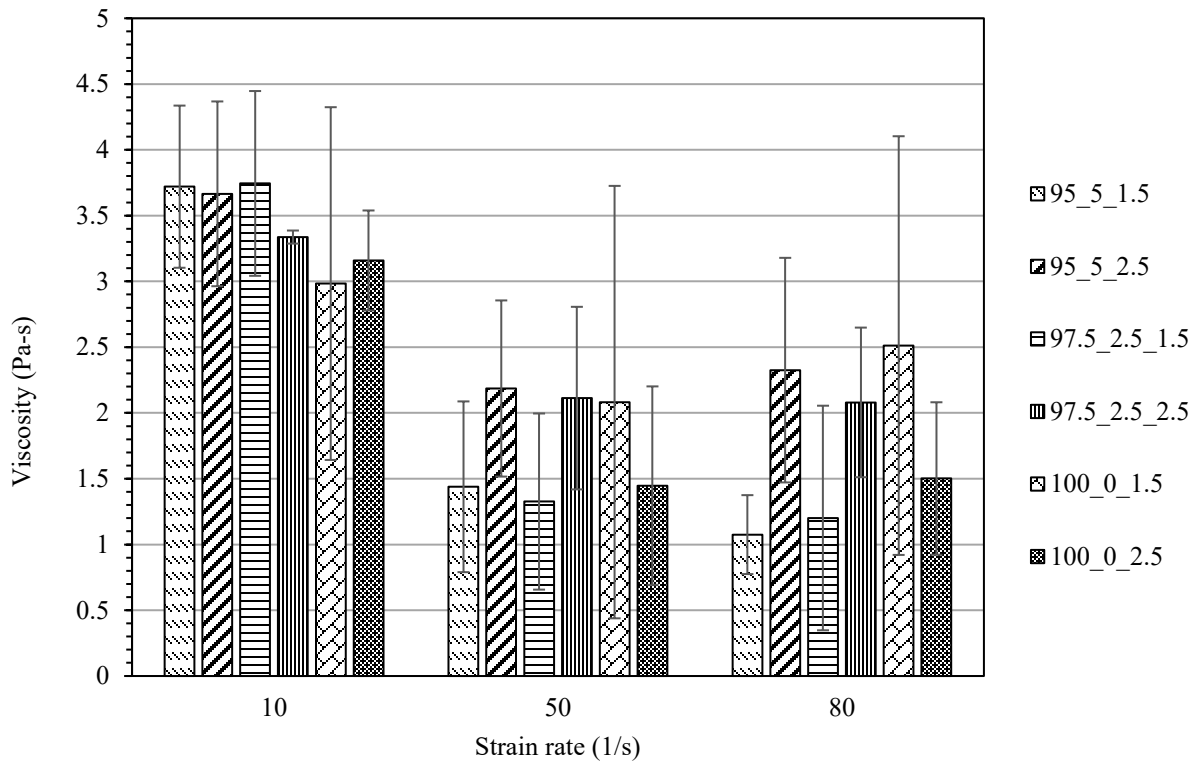
Figure 11. Apparent viscosities of the mixtures at the shear rates 10, 50, and 80 (1/s)

Figure 11 shows how the apparent viscosity of the mixture has reduced as the shear rate increases. With the higher shear rate, the mixtures become thin and less viscous desired for smooth extrusion. The experiments were designed with increasing shear rates in the rheometer so that they can be correlated to the pressure developed inside the extruder while printing. This pressure extrudes the cement mixture out of the nozzle. If the cement mixture does not possess a tight adhesion, the accumulating pressure caused the silica fume and water molecules to extrude, leaving the cement and SP inside the extruder. This is detrimental since the extruded material contained only silica fume and water. Once all the water got extruded, the cement and SP stayed inside, thus blocking the nozzle. This could be avoided by identifying the best proportion of solid additives with higher cohesion (tightly packed ingredients).

When the mixture particles breakdown during the loading cycle, the mixture loses the yield stress. However, the experimental results (Table 2) indicated that the yield stress of the samples did not display a steady increment with the addition of both silica fume and SP since the resting time (Dwell time) 60 seconds was not sufficient for the mixtures to regain the yield stress lost during the loading cycle. Schwartzentruber et al. [49] reported that the yield stress of the concrete mixture increased with the resting time after shearing. Thus, the mixtures with higher SP and silica fume need more resting time to regain the yield stress.

The thixotropy also played a significant role in the viscosity of the mixture. Higher the thixotropy of the mixture, higher is the energy required to breakdown the ingredients/particles. When the structural breakdown occurred faster, the mixture became less viscous. The addition of silica fume and SP helped the mixtures to re-coagulate faster, which could be seen by the increasing viscosity values in Table 2. However, this faster re-coagulation was not always desired for 3D printing by extrusion since the concrete mix with higher SP and silica fume would cure rapidly sometimes inside the extruder. Hence it is crucial to determine the proportion of additives as both insufficient as well as overdosage affected the thixotropy of the mixture and had their impacts on the viscosity and the yield stress of the mixtures.

The sample mixtures were 3D printed using the printer in the lab to check the buildability and extrudability. All the mixtures were printed separately into a 4x4 inches square wall. Based on the extrudability and buildability a discussion chart has been created (Table 3). Mixtures with higher yield stress started crunching the layers beneath whereas the mixture with less yield stress did not stack up in layers.

Table 2. Yield stress, thixotropic loop area, and Bingham viscosity measured from rheograms.

Mixtures (C_SF_SP)	95_5_1.5	97.5_2.5_1.5	100_0_1.5	95_5_2.5	97.5_2.5_2.5	100_0_2.5
Yield stress (Pa/s)	28.63	27.83	39.01	41.19	11.57	2.24
Thixotropic loop area	85.99	534.9	2874.4	451.24	230.1	583.32
Bingham viscosity (Pa)	0.63	0.66	1.98	1.1	1.91	2.23

Table 3. Printability discussion

Mixture	Printed Structure	Discussion on Printability
95C_5SF_1.5SP		Has the highest proportion of silica fume, highly cohesive mixture, has slower restructuration rate, the mixture cures slowly and retains the desired viscosity for printing for a long time, has high yield stress and as printed it suppresses the layers beneath thus affecting the layer heights
95C_5SF_2.5SP		Due to higher SP content, they are less viscous than the mixture above, has slightly higher restructuration rate and does not retain the printable viscosity for a long time as the previous one, cures faster in the extruder due to higher restructuration capability
97.5C_2.5SF_1.5SP		This mix has the appropriate silica fume and SP for printing and stacking the layers. As seen from the rheological assessment, they possess similar viscosity and yield stress as the 1st mix. They regain the yield stress slowly and hence while printing they do not affect the layers below
97.5C_2.5SF_2.5SP		This mixture is less viscous and has higher restructuration due to higher SP content, they do not hold the desired viscosity for printing for a long time as they cure faster. Since they regain their yield stress as time increases, the layers will compress while curing
100C_0SF_1.5SP		With no silica fume, this is the weakest of all the six mixtures, they have higher thixotropy and are less cohesive. Since they need more time to regain the yield stress, they are so weak and do not possess enough strength to hold the layers up
100C_0SF_2.5SP		As seen from the rheological assessment, at higher shear rates (during extrusion) they become less viscous, yet they have the highest restructuration rate of all the six mixtures. Since they are less viscous, they are not suitable for printing instantly

After analyzing the rheological results and the printability of the mixtures, the samples with appropriate yield stress and viscosity have been identified and are highlighted in the table above. The highlighted samples demonstrated better extrudability (holding the desired viscosity to print for a long time) and buildability ability to stack up layers without crushing the layers beneath). Using the same mixtures several other structures were 3D printed which can be seen in figure 12 below.
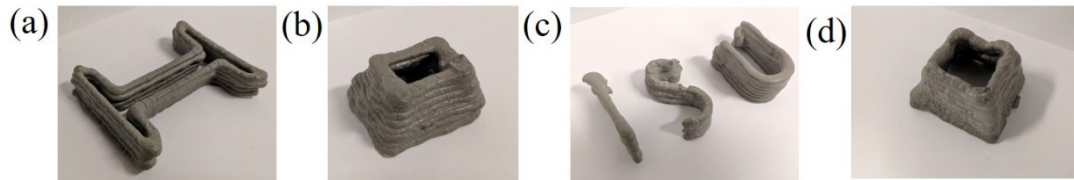
Figure 12. 3d printed concrete structures

4.2.Compression Test Results

The compression tests made on the sample mixtures is shown in figure 13. The compression strength of the mixture increases with the increase in admixtures. Both Silica Fume and Superplasticizer improved the strength of the mixture. Hence the admixtures are beneficial in any proportion rather than printing the raw cement. Printing raw cement with no additives caused immediate cracks in the constructs.
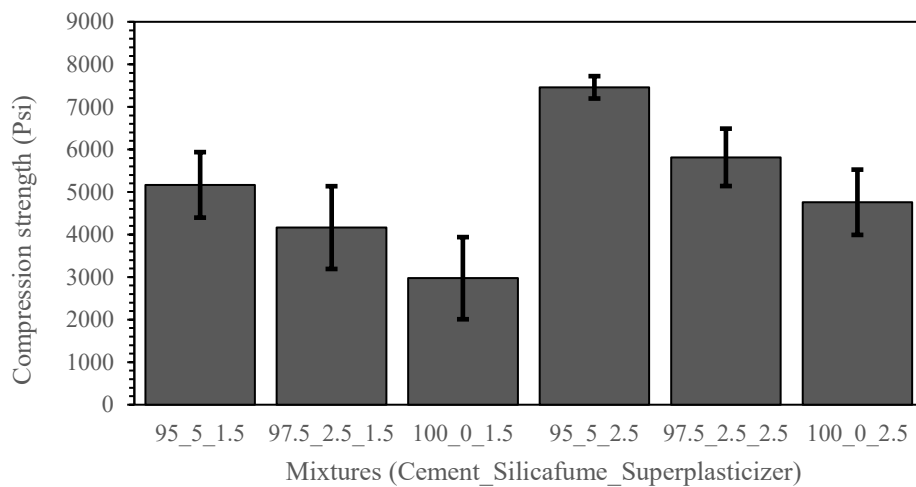
Figure 13. Apparent viscosities of the mixtures at the shear rates 10, 50, and 80 (1/s)

CHAPTER 5. STUDY EFFECTS OF NOZZLE GEOMETRIES: QUANTIFYING CONTOUR DEVIATION AND MECHANICAL PROPERTIES

As mentioned earlier, DIW uses a nozzle to extrude the printable ink, the geometry of the nozzle directly affects the geometry of the filament. Research works have been conducted on different additive printing techniques using different construction materials from clay to cement, to study the impacts of printing parameters such as speed, time, curing temperature, and proportion of chemical additives [50-56]. This study is focused on analyzing the effects of nozzle geometries in the 3D printed constructs.

For example, a cylindrical part that is printed with a circular nozzle has a round edge (see figure 14. a) in each layer, whereas the same part when printed with a square or rectangular nozzle has a flat edge (see figure 14. b). Since additive printing is a layer-after-layer approach, the geometry of each layer contributes to the overall surface finish of the printed constructs. As a result, it is essential to pre-determine the nozzle geometry to avoid the contour deviations that builds up through the layers.

The term "ready-to-print" denotes the fluidic properties such as viscosity, buildability, and yield stress, which are suitable for instantaneous printing. Previous research works [57-60] on construction materials suggest that the rheological behavior of the mixture plays a crucial role in printability and buildability. Research works also reported the necessity of printing parameters for 3D printing, how changing the printing parameters affects the buildability of the material [61-65]. Research work was conducted before, getting a perfectly rectangular block using a rectangular extruder by tweaking the printing parameters and extruder structures using iterative approach [66]. Researchers have worked to improve the surface finish of the printed constructs by reducing the layer heights [67] but reducing the printing speed or layer height increased the production time. It

was reported that generally using an elliptical nozzle for printing caused bulky curvatures near the edges on the printed structures [68].

To study the contour deviations and changes in mechanical properties while using different nozzle geometries, commercially available ready-to-print Prai-3D stoneware clay has been used to print the structures using a DIW printer and tested. Section 5.1 will explain the process involved in preparing the clay materials for 3D printing, including the clay properties. This section also describes the curing process. Section 5.2 will explain the printing parameters, and the visual representation of parts printed using different nozzle geometries. Sections 5.3 - 5.6 will have the procedure for mechanical testing made on the 3D printed constructs and methods used for quantifying the contour deviations and surface roughness. The results of the tests are discussed and summarized in chapter 6.
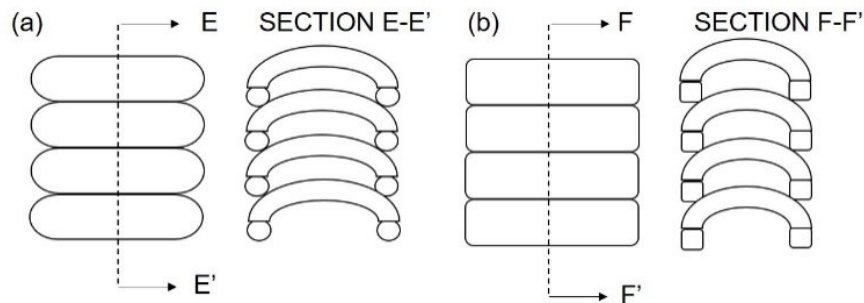
Figure 14. Cylinder when printed with (a) circular nozzle and (b) square nozzle

5.1.3D Printing Clay Constructs

PRAI–3d stoneware clay [69] for 3D printing was purchased from 3DPotter Inc. The purchased clay was mixed with water -to-clay (w/c) 0.3 weight proportion and set aside at room temperature for 12 hours. The clay is pre-prepared and de-aired when purchased from the manufacturer, and hence the hydrated clay is directly loaded into the extruder of the printer. A 3D Potterbot 7 Super printer, which is a DIW machine, was used to 3D print the samples.

The Potterbot used in this research was controlled by the Repetier host software. The 3D CAD model of a cylinder was imported, and the tool path for the printer was generated as G- Code from the software. This G-Code is the pattern in which the Potterbot extruder printed the clay onto the substrate.

5.2.3D Printing Parameters

For this study, cylindrical samples were printed on 3d potter bot super 6 printer using nozzles with 1) circular and 2) square outlet geometries see figure 15. A 3D CAD model of a 2x1 inch (height-by-diameter) cylinder was made and the G-code was generated with all the printing parameters kept constant. The following printing parameters were used:

1)   Printing speed = 15 mm/s

2)   Circular nozzle diameter = 6 mm

3)   Square nozzle size = 6x6 mm

4)   Infill = 0.8 on 1

5)   Extrusion speed = 20 mm/s

All the printed cylindrical samples were cured at the room temperature for 72 hours and then sintered in a hot plate at 100 °C for 24 hours.
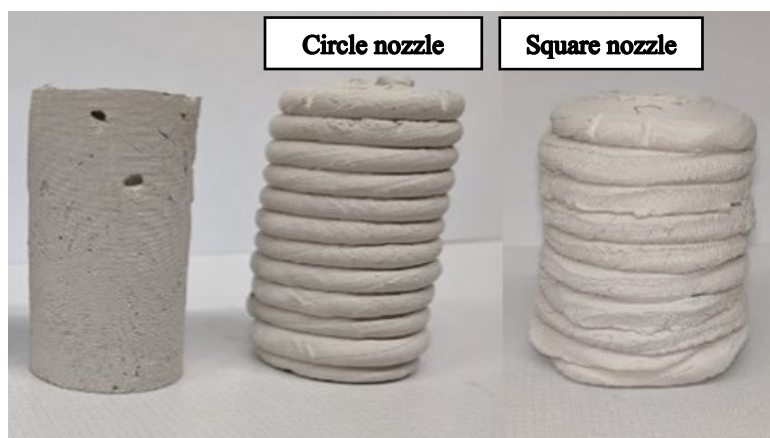

Figure 15. 3D printed cylinders and clay mold

5.3. Mechanical Testing

The samples 3D printed with circular and square nozzles, although using the same 0.8 infill, the density of the construct differs. With the same 0.8 infill, the volume of clay in cylindrical samples, 3D printed with different nozzle varies. This difference in volume affects the mechanical properties of the printed constructs.

5.4. Compression Test on Regular Clay

The compression test is one of the most conventional tests used to characterize the mechanical properties of a mixture/ink. This test aims to determine the compressive strength of PRAI 3D stoneware clay so that it can be used to conduct a comparative study with the compression strength of 3D printed clay constructs. To determine the compressive strength of clay, two cylindrical molds (2x1 inch) were 3D printed using Uprint, a Fused Deposition Modeling (FDM) polymer printer, and the molds are filled with the clay and compacted. The molds were stripped off after curing for 72 hours with a tolerance of ±2 hours at room temperature, and the specimens were sintered in a hot plate at 100 °C for 24 hours before testing. The samples were loaded in the Shimadzu UH-F300kNX hydraulic universal testing machine (UTM) until failure without any shock loading. The ultimate load until failure was noted for clay samples and was used to calculate the compression strength of the samples using the following equation (3). Two clay samples were tested, and a type 3 "columnar vertical cracking with no cones" type of failure was noted on both the samples.

5.5. Compression Test on Printed Constructs

A set of two samples each for both square and cylindrical nozzles were 3D printed. The printed cylinders were cured and sintered in the same way as the regular clay mold and are loaded into the UTM machine. The top and the bottom surfaces of the 3D printed samples were

smoothened before loading, and the maximum load until failure was noted. Using the same equation, the compression strength of all the four samples were noted.
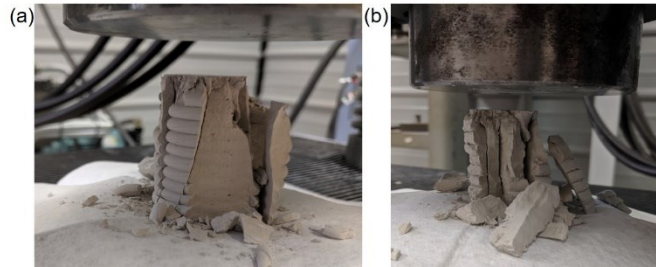

Figure 16. Compression test performed on 3D printed parts (a) printed with a circular nozzle and (b) printed with a square nozzle

5.6.Contour Deviation

As discussed in figure 14, using different nozzle geometry for printing affects the contour of the 3D printed part. The purpose of the study in this section is to scan the cylinders printed with circular and square nozzles and compare them with the regular CAD file of the cylindrical part to determine the contour deviations.

The structured light system (SLS) is an extension of stereo vision. The difference is that the latter uses two cameras whereas the former uses a projector and a camera for acquiring the 3D information of the object. However, correspondence detection using stereo vision becomes difficult in the case of objects with uniform or repetitive texture. To solve this problem, SLS uses a projector in place of one of the two cameras.

5.6.1.   SLS Scanning

Figure 17. represents the principle of the structured light system. Here A represents a projector pixel, C represents a camera pixel, and the B is the object point being scanned. The projector projects codified fringe patterns on the object. The projected fringe patterns will get distorted because of the surface variations in the object, and this image (an object with distorted fringe patterns) is captured by the camera. Using the codifications in the fringe patterns, the

correspondence. The scanning and reconstruction of the 3D printed constructs followed the procedures from [70] and the calibration method from [71] has been used to finally reconstruct the 3D geometry.
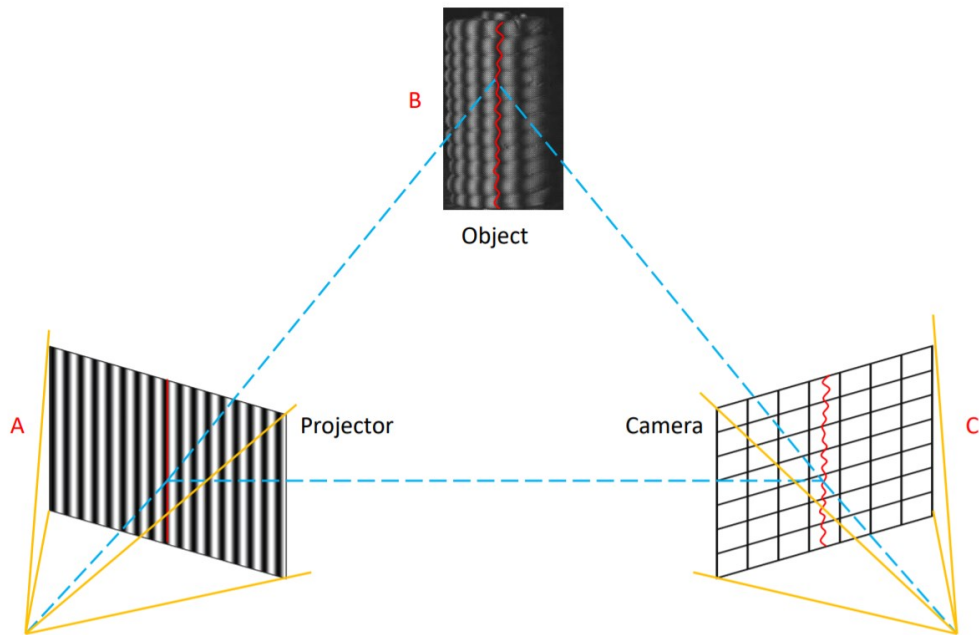
Figure 17. Schematic representation structured light scanning (SLS) system

5.6.2. Experiment Setup of 3D Scanning

The experimental setup consists of a digital light processing projector (LightCrafter 4500) for pattern projection, a complimentary-metal-oxide-semiconductor (CMOS) camera (model: FLIR Grasshopper3 GS3-U3-41C6C-C) for image acquisition and an external trigger for synchronizing the camera and projector. The projector resolution was set to 912×1140 pixels whereas the camera resolution was set to 1280×960 pixels. The image acquisition rate was set to 166 Hz. We have used three-step phase-shifted patterns for phase retrieval and another set of three-step phase-shifted binary dithered patterns for phase unwrapping.

5.6.3. Data Processing of Point Cloud

The SLS system was used to scan the samples all around in three rotations (3 poses at 120º through each rotation) so that the entire surface of the printed sample is reconstructed. The point cloud data obtained from the samples are compared with the STL file of the regular cylinder. CloudCompare software [72] was used for comparing the point-cloud analysis and to determine the overall deviation of the printed sample from the regular cylinder. A standard procedure was maintained to perform this analysis which is shown in the flow chart below (Figure 18.)
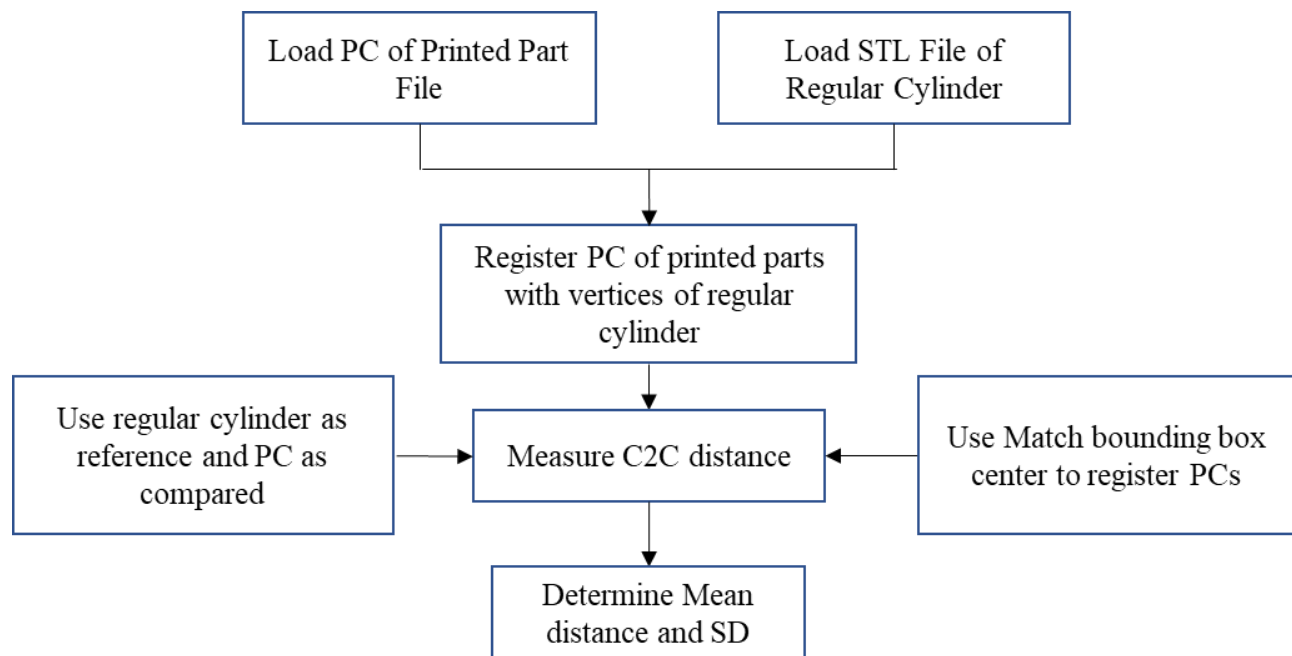
Figure 18. Flow chart showing the procedure used to compare the point cloud and data processing in CloudCompare.

5.6.4. Data Analysis

The mean distance and the standard deviation (SD) obtained from each pose of the sample using CloudCompare analysis were used to compute the overall mean distance which denotes the deviation in the printed samples from the regular cylinder. This overall mean distance is the difference in mm from the printed samples to the regular cylinder. Apart from this cloud-to-cloud

30

mean distance deviation, the surface roughness of the samples was computed using the point cloud

data. Figure 19 shows the step by step procedure involved in the CloudCompare simulation.

Figure 19. Step-by-step procedure involved in the CloudCompare simulation to evaluate contour deviation

CHAPTER 6.   RESULTS AND DISCUSSIONS ON NOZZLE STUDY

The compression test results in Figure 20. shows that the cylindrical samples printed with square nozzle have higher compression strength than the samples printed with a circular nozzle. Th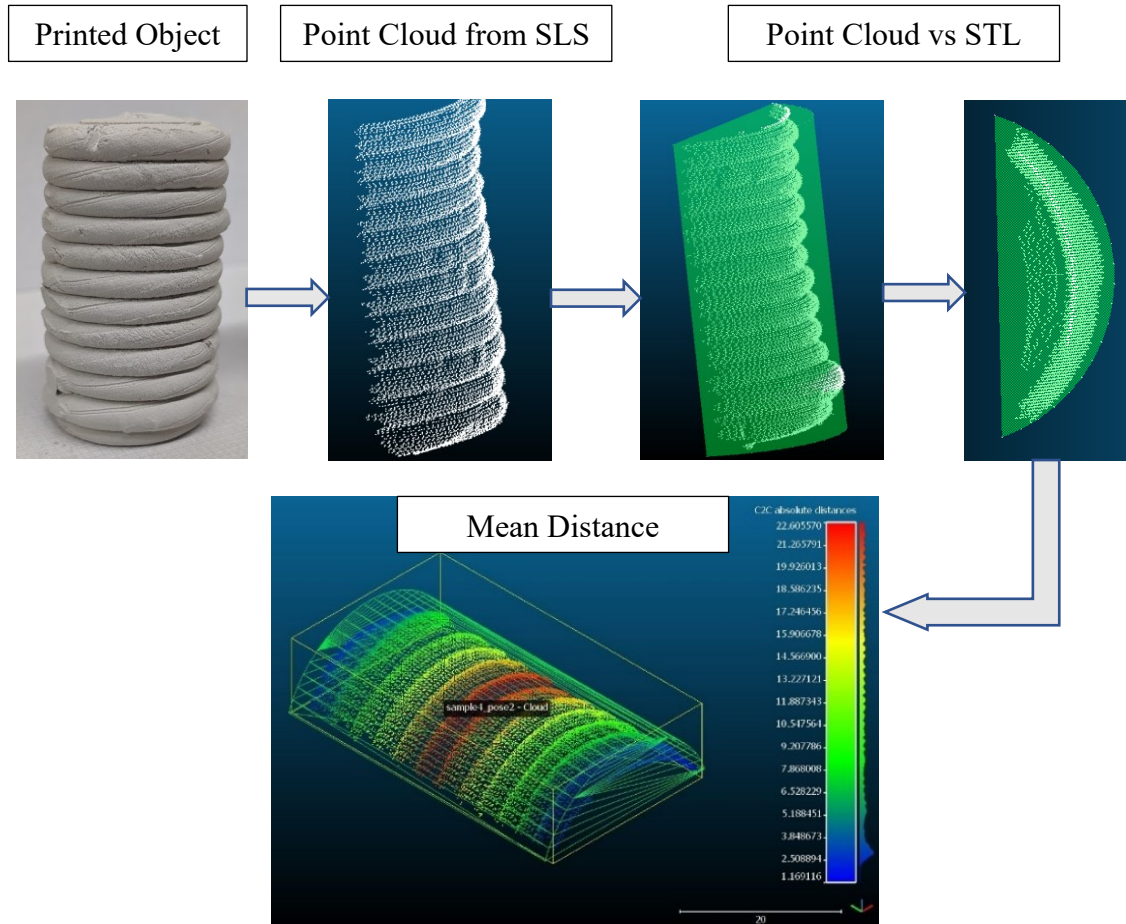e extrusion system used in the study is pressure-actuated and the pressure exerted by the extruder remains constant for both the nozzle geometries. In such a case, square nozzle extrudes a higher volume of clay per layer than the circular nozzle, and hence the compression strength of the sample is higher. Interestingly, the compression strength of the 3D printed samples is higher than the regular cylindrical casts despite the infill set to 0.8 on 1. This is because the compacted clay inside the mold has no way to expand and while curing, also the samples lost their water content during the sintering process, and hence the size of the cured part reduced. Whereas the printed samples are not confined into any molds and are free for expansion right after printing. This difference in the sizes of the printed parts and the casted cylinders affected the compression strength.

The surface roughness of the samples measured from the SLS system shows that the samples printed with square nozzle exhibit high Ra and Rq values (see Figure 21.). Since the square nozzle generates more deviation through every layer than the circular nozzle, the surface roughness is very high for them. The point cloud analysis result shows that the cylindrical samples printed with a circular nozzle have lesser cloud-to-cloud mean distance and SD when compared with the square nozzle. This is obvious as the circular nozzle prints more uniform curvature than the square nozzles. The cloud-to-cloud mean distance is very high for the samples printed with the square nozzle as the square nozzle creates twists on the contour surface. Hence the contour deviations are higher when the cylinders are printed with square nozzles. Figure 22 shows the mean distance between cloud-to-cloud points.
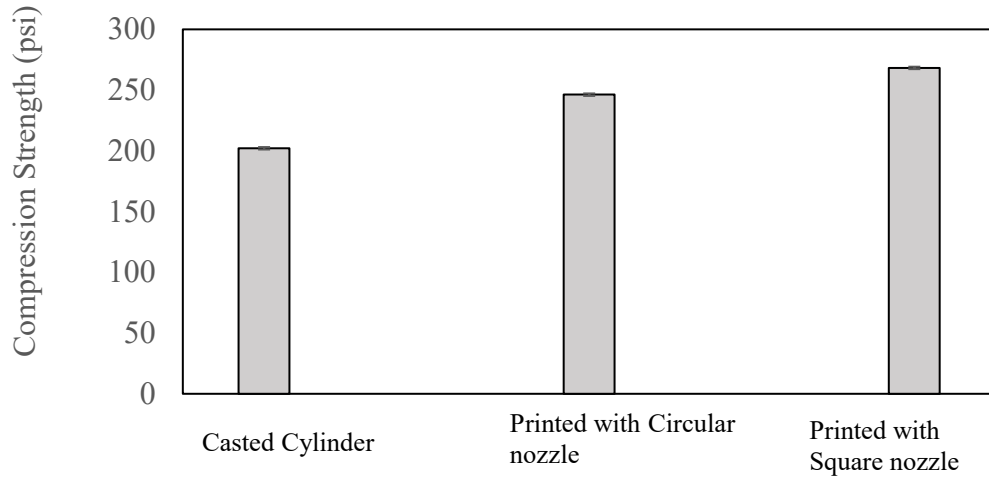
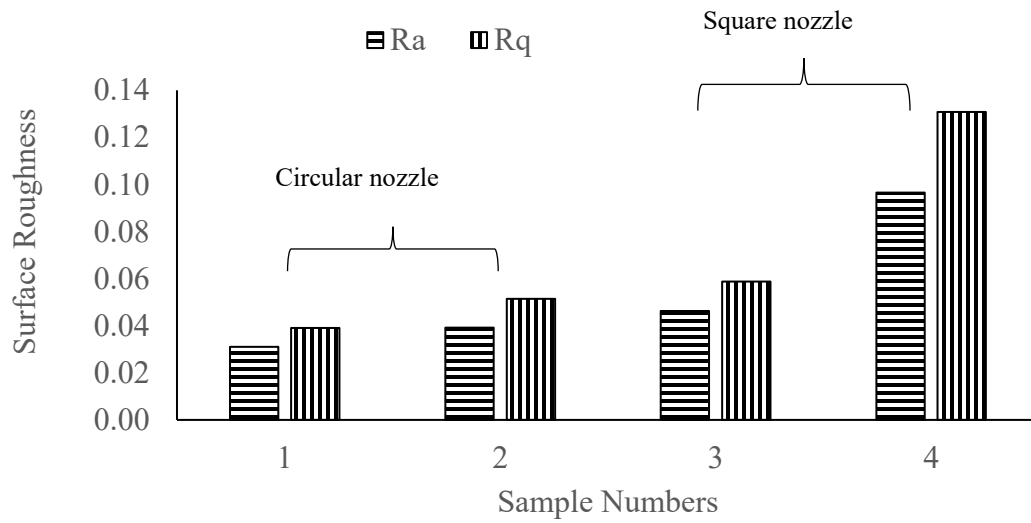Figure 20. Compression test results showing the compression

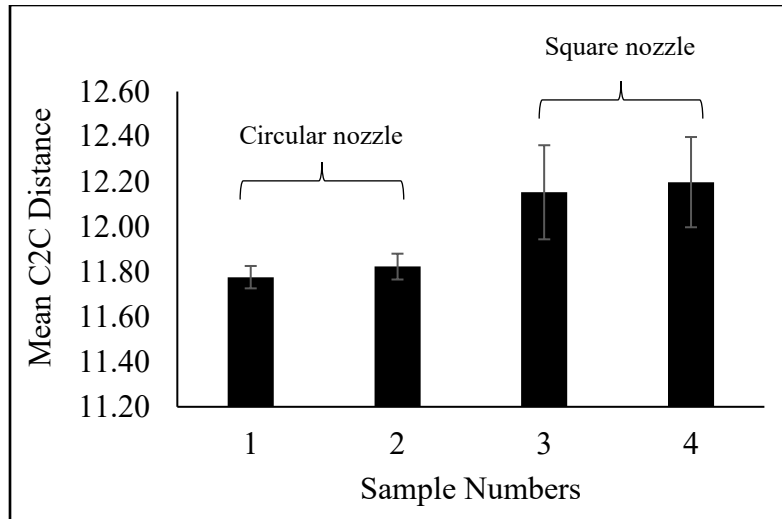Figure 21. Surface roughness of the samples measured from the SLS system

Figure 22. Mean c2c distances results from CloudCompare simulation

Based on the three parameters, although the square nozzle imparts higher compression strength naturally, the surface roughness and the mean deviation is very higher. Also, the compression strength of the samples printed with a circular nozzle inhibits better mechanical properties with a smooth surface finish and lesser contour deviations from the CAD model. Hence for cylindrical objects, it is better to go for a circular nozzle rather than the square nozzle. For structures like columns or walls, square nozzles would work better than the circular nozzle as they can be printed with linear or parallel tool pathing which will not result in twists in the layers. The next stage of this research work will continue testing the same parameters for non-cylindrical, free form constructs.

In this study, three parameters namely compression strength, surface roughness, and cloud-to-cloud mean distance were used to quantify the contour deviations and mechanical properties of the clay samples printed with circular and square nozzles. Using the SLS system, the printed samples were scanned, and the point-cloud data generated from the system was compared with the CAD model to determine the contour deviations. The surface roughness of the printed constructs determined shows how critical it is to pre-determine the nozzle geometry before printing, as in this

case, cylindrical construct had large contour deviation when printed with a square nozzle than the circular nozzle. Although using a square nozzle increases the compression strength of the constructs by improving the density, it cannot be traded off for the external surface finish. Using the same parameters, the deviations and mechanical properties of the free form constructs can be determined which will be the future work from this research background.

CHAPTER 7.   SUMMARY AND FUTURE WORKS

To summarize the research, in the first study, fresh concrete mixtures were 3D printed and their flow properties were characterized based on their rheological properties. The additives, silica fume added to the concrete mixture improved the yield stress and Superplasticizer helped maintain the desired viscosity of the concrete mix for 3D printing. The proportions of the admixtures in the cement have a direct impact on the printability and buildability of concrete mixture. A mixture with higher yield stress is desired for stronger constructs, but they were not suitable for 3D printing as the layers could not stack up and compress the layers beneath while printing. Similarly, a mixture with higher viscosity would cure faster but needs higher extrusion pressure. Hence an appropriate proportion of additives suitable for printing and building has been identified, based on the rheological tests and printability tests. Thixotropy of the concrete mixtures has been used to predict the printability of the mixture as the hysteresis loop area dictates the viscosity, yield stress, and the restructuration capability of the mixtures. Future work for this study will focus on shape fidelity and strength of the printed constructs with various print speed, nozzle geometries, and other additives. To scale up the 3D printing of concrete structures, like Big Area Additive Manufacturing (BAAM) on the construction field, flow properties of the concrete mixtures along with aggregates like fly ash, fiber composites, and waste plastics can be studied in the same manner followed in this research.

In the nozzle effects study, the importance of the nozzle geometry has been identified. The nozzle shape determines the shape of the filament, which further affects the contour of the construct. In the 3D printing process, nozzle selection is crucial since a proper nozzle geometry can reduce the surface unevenness and the stair-casing effects. In the research work, for cylindrical

constructs square nozzle created twists in the layers and the cylindrical nozzle created even contour.

Using the parameters namely compression strength, mean c2c distance, and the surface roughness, the deviations and mechanical properties of the other free form constructs such as walls, columns, etc., can be determined which will be the future work from this research background. This research work will serve as a guideline for nozzle geometry selection in 3D printing for civil infrastructures.

REFERENCES

[1] K.N. Jha, Formwork for Concrete Structures, Tata McGraw Hill Education Private Limited, New Delhi, ISBN (13): 978-1-25-900733-0, (2012)

[2] N. Lawson, I. Douglas, S. Garvin, C. McGrath, D. Manning, J.J.E.M. Vetterlein, Health, Recycling construction and demolition wastes–a UK perspective, Environmental Management and Health, 12 (2001), pp. 146-157

[3] The United States Environmental Protection Agency (EPA) report. [last accessed 19 June 2019]. www.epa.gov/smm/sustainable-management-construction-and-demolition-materials,

[4] United States Department of Labor Occupational Safety and Health Administration (OSHA) report, https://www.osha.gov/oshstats/commonstats.html, [last accessed 18 June 2019]

[5] M. Taylor, S. Wamuziri, I. Smith, Automated construction in Japan, Proceedings of the Institution of Civil Engineers-Civil Engineering, 156 (2003), pp. 34-41

[6] F. Bos, R. Wolfs, Z. Ahmed, T.J.V. Salet, P. Prototyping, Additive manufacturing of concrete in construction: potentials and challenges of 3D concrete printing, Virtual and Physical Prototyping, 11 (2016), pp. 209-225

[7] Hager, I., Golonka, A., & Putanowicz, R. (2016). 3D printing of buildings and building components as the future of sustainable construction. Procedia Engineering, 151, 292-299

[8] Panda, B., & Tan, M. J. (2018). Experimental study on mix proportion and fresh properties of fly ash-based geopolymer for 3D concrete printing. Ceramics International, 44(9), 10258-10265

[9] Khoshnevis, B., Hwang, D., Yao, K. T., & Yeh, Z. (2006). Mega-scale fabrication by contour crafting. International Journal of Industrial and Systems Engineering, 1(3), 301-320

[10] Nerella, V. N., Krause, M., Näther, M., & Mechtcherine, V. (2016). CONPrint3D—3D printing technology for onsite construction. Concrete in Australia, 42(3), 36-39

[11] Gosselin, C., Duballet, R., Roux, P., Gaudillière, N., Dirrenberger, J., & Morel, P. (2016). Large-scale 3D printing of ultra-high performance concrete–a new processing route for architects and builders. Materials & Design, 100, 102-109

[12] C. Hinczewski, S. Corbel, T. Chartier, Stereolithography for the fabrication of ceramic three-dimensional parts, Rapid Prototype. J. 4 (3) (1998) 104–111

[13] F. Liang, Y. Liang, Study on the status quo and problems of 3D printed buildings in China, Glob. J. Hum. Soc. Sci. 14 (5) (2014) 7–10

[14] I. Gibson, T. Kvan, L.W. Ming, Rapid prototyping for architectural models, Rapid Prototype. J. 8 (2) (2002) 91–95

[15] Lim, S., Buswell, R. A., Le, T. T., Austin, S. A., Gibb, A. G., & Thorpe, T. (2012). Developments in construction-scale additive manufacturing processes. Automation in construction, 21, 262-268

[16] A. Dubois, L.E. Gadde, Supply strategy and network effects – purchasing behavior in the construction industry, Eur. J. Purch. Supply Manag. 6 (3-4) (2000) 207–215

[17] https://www.bca.gov.sg/BuildableDesign/ppvc.html

[18] Perkins, I. and Skitmore, M., 2015. Three-dimensional printing in the construction industry: a review. International Journal of Construction Management, 15 (1), 1–9

[19] Moon, J., Grau, J. E., Knezevic, V., Cima, M. J., & Sachs, E. M. (2002). Ink-jet printing of binders for ceramic components. Journal of the American Ceramic Society, 85(4), 755-762

[20] Dini, E., 2009. D-SHAPE – The 21st-century revolution in building technology has a name. p. 1–16

[21] Nan, C., 2015. A new machine craft: a critical evaluation of architectural robots. In: Computer-aided architectural design futures. The next city – new technologies and the future of the built environment, CAAD futures 2015, international conference on computer-aided architectural design futures. Sao Paulo, Brazil, 422–438

[22] Wolfs, R. R. (2015). 3D printing of concrete structures

[23] Nerella, V. N., Krause, M., Näther, M., & Mechtcherine, V. (2016, June). Studying printability of fresh concrete for formwork free Concrete on-site 3D Printing technology (CONPrint3D). In Proceeding for the 25th conference on the rheology of building materials

[24] Tay, Y. W. D., Panda, B., Paul, S. C., Noor Mohamed, N. A., Tan, M. J., & Leong, K. F. (2017). 3D printing trends in the building and construction industry: a review. Virtual and Physical Prototyping, 12(3), 261-276

[25] Le, T. T., Austin, S. A., Lim, S., Buswell, R. A., Law, R., Gibb, A. G., & Thorpe, T. (2012). Hardened properties of high-performance printing concrete. Cement and Concrete Research, 42(3), 558-566

[26] Le, T. T., Austin, S. A., Lim, S., Buswell, R. A., Gibb, A. G., & Thorpe, T. (2012). Mix design and fresh properties for high-performance printing concrete. Materials and Structures, 45(8), 1221-1232

[27] Zareiyan, B., & Khoshnevis, B. (2017). Effects of interlocking on interlayer adhesion and strength of structures in 3D printing of concrete. Automation in Construction, 83, 212-221

[28] Panda, B., Mohamed, N. A. N., & Tan, M. J. (2018, April). Effect of 3d printing on mechanical properties of fly ash-based inorganic geopolymer. In International Congress on Polymers in Concrete (pp. 509-515). Springer, Cham

[29] Panda, B., Paul, S. C., & Tan, M. J. (2017). Anisotropic mechanical performance of 3D printed fiber-reinforced sustainable construction material. Materials Letters, 209, 146-149

[30] Freek Bos, Rob Wolfs, Zeeshan Ahmed & Theo Salet (2016) Additive manufacturing of concrete in construction: potentials and challenges of 3D concrete printing, Virtual and Physical Prototyping, 11:3, 209-225, DOI: 10.1080/17452759.2016.1209867

[31] Wolfs, R.J.M. (2015), "3D printing of concrete structures", MSc thesis, Eindhoven University of Technology

[32] Y. Weng, M. Li, M.J. Tan, S. Qian, Design 3D printing cementitious materials via Fuller Thompson theory and Marson-Percy model, Construction and Building Materials, 163 (2018), pp. 600-610

[33] K. Biswal, S.C. Sadangi, Effect of Superplasticizer and Silica Fume on Properties of Concrete, International Journal on Civil and Environmental Engineering, 1 (1), pp. 41-43

[34] J. Gołaszewski, J. Szwabowski, Influence of superplasticizers on the rheological behavior of fresh cement mortars, Cement and Concrete Research, 34 (2004), pp. 235-248

[35] T.H. Phan, M. Chaouche, M. Moranville, Influence of organic admixtures on the rheological behavior of cement pastes, Cement and Concrete Research, 36 (2006), pp. 1807-1813

[36] P.K. Mehta, P.J. Monteiro, Concrete Microstructure, Properties and Materials, McGraw-Hill Publishing, (2017)

[37] A. Ramezanianpour, A. Kazemian, M. Nikravan, A. Mahpur, M. Moghadam, Influence of a low-activity slag and silica fume on the fresh properties and durability of high-performance self-consolidating concrete, Proceedings of 3rd International Conference on Sustainable Construction Materials and Technologies, Kyoto, Japan (2013)

[38]

[39] ASTM C39 / C39M-20, Standard Test Method for Compressive Strength of Cylindrical Concrete Specimens, ASTM International, West Conshohocken, PA, 2020, www.astm.org

[40] ASTM C192 / C192M-19, Standard Practice for Making and Curing Concrete Test Specimens in the Laboratory, ASTM International, West Conshohocken, PA, 2019, www.astm.org

[41] Cyr, M., Legrand, C., & Mouret, M. (2000). Study of the shear thickening effect of superplasticizers on the rheological behavior of cement pastes containing or not mineral additives. Cement and Concrete Research, 30(9), 1477-1483

[42] Kim, J. H., Kwon, S. H., Kawashima, S., & Yim, H. J. (2017). Rheology of cement paste under high pressure. Cement and Concrete Composites, 77, 60-67

[43] Björnström, J., & Chandra, S. (2003). Effect of superplasticizers on the rheological properties of cement. Materials and Structures, 36(10), 685-692

[44] Khayat, K. H., Saric-Coric, M., & Liotta, F. (2002). Influence of thixotropy on stability characteristics of cement grout and concrete. Materials Journal, 99(3), 234-241

[45] Ferrari, L., Kaufmann, J., Winnefeld, F., & Plank, J. (2011). A multi-method approach to study the influence of superplasticizers on cement suspensions. Cement and Concrete Research, 41(10), 1058-1066

[46] Banfill, P. F. G. (1990). Rheology of Fresh Cement and Concrete: Proceedings of an International Conference, Liverpool, 1990. CRC Press

[47] T.M. Salem, Electrical conductivity and rheological properties of ordinary Portland cement–silica fume and calcium hydroxide–silica fume pastes, Cement and Concrete Research, 32 (2002), pp. 1473-1481

[48] N.B. Ur'ev, R. Baru, A. Izhik, S. Choi, V. Saskovets, (1997). Rheology and thixotropy of cement-water suspensions in the presence of superplasticizers, Colloid Journal of the Russian Academy of Sciences, 59.6 (1997), pp. 773-779

[49] V. Petkova, V. Samichkov, Some influences on the thixotropy of composite slag Portland cement suspensions with secondary industrial waste, Construction and Building Materials, 21 (2007), pp. 1520-1527

[50] L.D. Schwartzentruber, Amp, Apos, Aloia, R. Le Roy, J. Cordin, Rheological behavior of fresh cement paste formulated from a Self Compacting Concrete (SCC), Cement and Concrete Research, 36 (2006), pp. 1203-1213

[51] Lima, P., Zocca, A., Acchar, W., & Günster, J. (2018). 3D printing of porcelain by layer-wise slurry deposition. Journal of the European Ceramic Society, 38(9), 3395-3400.

[52] Faes, M., Valkenaers, H., Vogeler, F., Vleugels, J., & Ferraris, E. (2015). Extrusion-based 3D printing of ceramic components. Procedia Cirp, 28, 76-81

[53] El Idrissi, H. E. B., Daoudi, L., El Ouahabi, M., Collin, F., & Fagel, N. (2018). The influence of clay composition and lithology on the industrial potential of earthenware. Construction and Building Materials, 172, 650-659

[54] Perrot, A., Rangeard, D., & Courteille, E. (2018). 3D printing of earth-based materials: Processing aspects. Construction and Building Materials, 172, 670-676

[55] Friedman, J., Kim, H., & Mesa, O. (2014). Experiments in additive clay depositions. In Robotic Fabrication in Architecture, Art and Design 2014 (pp. 261-272). Springer, Cham

[56] Dunn, K., O'Connor, D. W., Niemelä, M., & Ulacco, G. (2016). Free Form Clay Deposition in Custom Generated Molds. In Robotic Fabrication in Architecture, Art and Design 2016 (pp. 316-325). Springer, Cham

[57] Rosenwasser, D., Mantell, S., & Sabin, J. (2017). Clay non-wovens: robotic fabrication and digital ceramics

[58] Paul, S. C., Tay, Y. W. D., Panda, B., & Tan, M. J. (2018). Fresh and hardened properties of 3D printable cementitious materials for building and construction. Archives of civil and mechanical engineering, 18(1), 311-319

[59] Wolfs, R. J. M., Bos, F. P., & Salet, T. A. M. (2019). Hardened properties of 3D printed concrete: The influence of process parameters on interlayer adhesion. Cement and Concrete Research, 119, 132-14

[60] Salet, T. A. M., & Wolfs, R. J. M. (2016). Potentials and challenges in 3D concrete printing.

[61] Tay, Y. W., Panda, B., Paul, S. C., Tan, M. J., Qian, S. Z., Leong, K. F., & Chua, C. K. (2016). Processing and properties of construction materials for 3D printing. In Materials Science Forum (Vol. 861, pp. 177-181). Trans Tech Publications.

[62] Wolfs, R., Salet, T., & Hendriks, B. (2015, August). 3D printing of sustainable concrete structures. In Proceedings of IASS annual symposia (Vol. 2015, No. 2, pp. 1-8). International Association for Shell and Spatial Structures (IASS)

[63] Holt, C., Edwards, L., Keyte, L., Moghaddam, F., & Townsend, B. (2019). Construction 3D printing. In 3D Concrete Printing Technology (pp. 349-370). Butterworth-Heinemann

[64] Buswell, R. A., Soar, R. C., Gibb, A. G., & Thorpe, A. (2007). Freeform construction: mega-scale rapid manufacturing for construction. Automation in construction, 16(2), 224-231

[65] Buswell, R. A., Soar, R. C., Gibb, A. G., & Thorpe, A. (2007). Freeform construction: mega-scale rapid manufacturing for construction. Automation in construction, 16(2), 224-231

[66] Perkins, I., & Skitmore, M. (2015). Three-dimensional printing in the construction industry: A review. International Journal of Construction Management, 15(1), 1-9

[67] Lao, W., Li, M., Masia, L., & Tan, M. J. (2017). Approaching Rectangular Extrudate in 3D Printing for Building and Construction by Experimental Iteration of Nozzle Design

[68] Luigi Maria Galantucci, Fulvio Lavecchia, and Gianluca Percoco. An experimental study aiming to enhance the surface finish of fused deposition modeled parts. CIRP Annals Manufacturing Technology, 58(1):189–192, 2009

[69] Khoshnevis, B. (2004). Automated construction by contour crafting—related robotics and information technologies. Automation in construction, 13(1), 5-19

[70] https://3dpotter.com/add-ons/prai

[71] Suresh, Vignesh, Yajun Wang, and Beiwen Li. "High-dynamic-range 3D shape measurement utilizing the transitioning state of the digital micromirror device." Optics and Lasers in Engineering 107 (2018): 176-181

[72] Li, Beiwen, Nikolaus Karpinsky, and Song Zhang. "Novel calibration method for a structured-light system with an out-of-focus projector." Applied Optics 53.16 (2014): 3415-3426
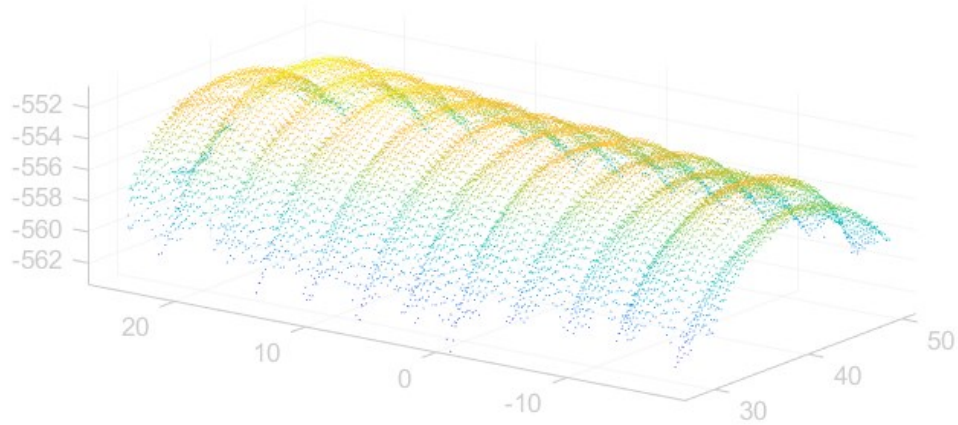
[73] https://www.cloudcompare.org/

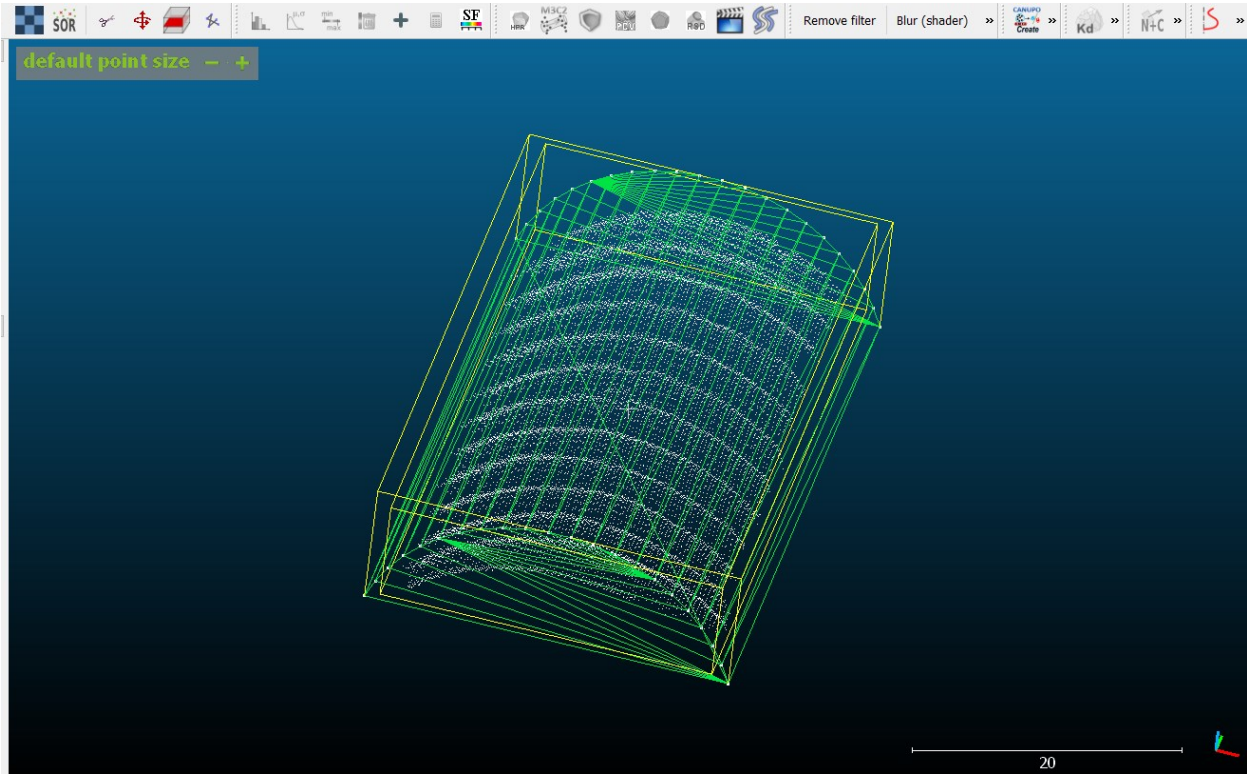## APPENDIX A.   CLOUD COMPARE SIMULATION

Reconstructed image of the scanned clay construct from the SLS system
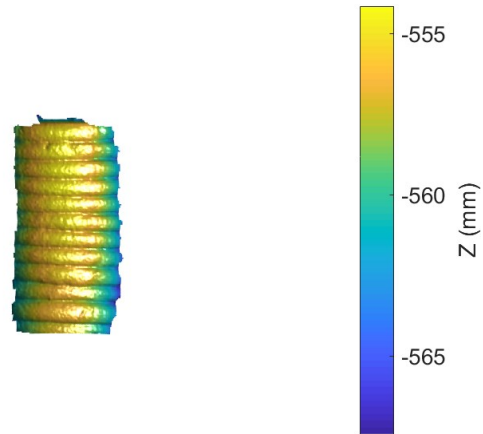
Point Clouds obtained from the SLS system

STL vertices and the Point Clouds of the printed constructs overlapped

APPENDIX B.   SURFACE ROUGHNESS EVALUATION

The surface roughness of the 3D printed samples was determined using the 2D plot obtained from the SLS scanning. The data points from the 2D plot are extracted as an array, and the peaks and valleys are counted. The array consists of numeric and non-numeric characters that are obtained from the 2D plot. The NaN (Not a Number) and Non-NaN values in the array of the sample were used to determine the Surface roughness and root mean square values of the samples.

MATLAB CODE:

```
A = importdata ('2dPlot_sample_1_pose_1.mat');%Sample# and
Pose# varies

plot (A); %Plots the 2D contour of the scanned sample#
pose#

isnan(A);%Counts the number of Nan's in the array A

Nans = sum(isnan(A)); %Sums up all the NaN in the array A

n = numel(A);%Returns the number of elements in A

Nonnans = n - Nans; %Returns the number of Non-Nan's in A

M = mean(A, 'omitnan'); %Returns the mean of the array
omitting the NaN's in the array A

A1 = A-M;

S = sum(abs(A1), 'omitnan');

Ra = S/Nonnans;%Returns the surface roughness value

Y = (A1.^2);

F = sum(Y, 'omitnan');

Z = F/Nonnans;
```

```
Rq = sqrt(Z); %Returns the root mean square value
```
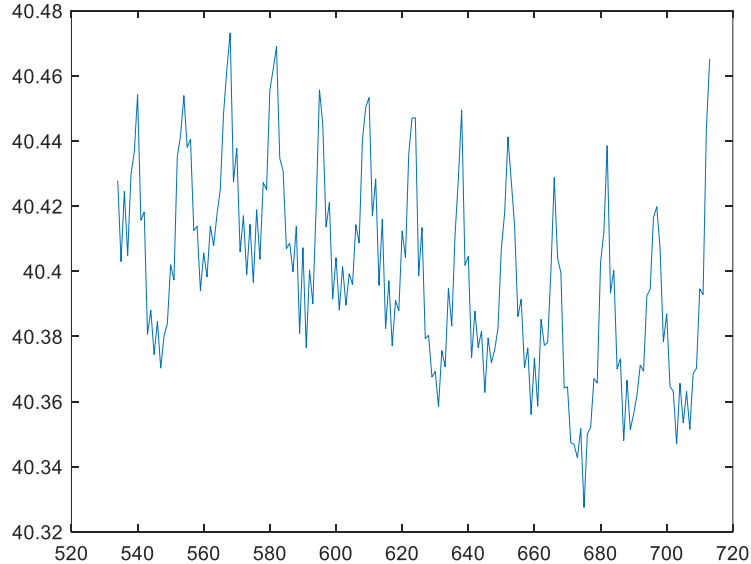
The average surface roughness and root mean square values are calculated from the arrays using the formula given below:

$$\text{Average Surface Roughness Ra} = \text{Center Line Average} = \frac{Average\ of\ all\ the\ values\ in\ the\ array}{Total\ number\ of\ values}$$

$$\text{Root mean square Rq} = \frac{\sqrt{sum\ of\ squares\ of\ the\ values\ in\ the\ array}}{\sqrt{Total\ number\ of\ values}}$$

Result:

2D Plot of Sample 1 Pose 1

R_a and R_q values evaluated from the Array for sample 1 pose 1

A	*1x1280 double*	
A1	*1x1280 double*	
ans	*1x1280 logical*	
F	0.5764	
M	39.4283	
n	1280	
Nans	1099	
Nonnans	181	
Ra	0.0423	
Rq	0.0564	
S	7.6619	
Y	*1x1280 double*	
Z	0.0032	